Dynamic Aspects of Cortical Rhythmic Activities

Tatsuichiro OHSHIO

Dept. Physics, Fac. Science, Kyoto University, Kyoto

Introduction

The purposes of this paper are (1) to provide a consistent explanation to account for electrical phenomena in EEG (electroencephalogram) as a manifestation of mass action in the nervous system[1], (2) to present some experiments for verifications of the theory, and (3) to propose a new experimental paradigm for a demonstration of the existence of short term "memory".

Mass Action in the Nervous System

Wilson and Cowan proposed the nonlinear differential equations for activities of localized neural mass[2]:

$$\tau_e \dot{E} + E = (1 - r_e E) S_e [c_{ee} E - c_{ei} I + P_e]$$
$$\tau_i \dot{I} + I = (1 - r_i I) S_i [c_{ie} E - c_{ii} I + P_i] \tag{1}$$

where e and i stand for excitation and inhibition; E and I for time coarsegrained excitatory and inhibitory activities; τ for neural membrane time constant; r for refractory period; $S[\cdot]$ for nonlinear response function; c for connectivity constant; and P for afferent input.

By a perturbational technique around the unstable singular point of eq. (1), some reductions can be made, at a low level of activities, to result in the FitzHugh type equations[3]:

$$\tau_1 \dot{E} = f(E) - I + P$$
$$\tau_2 \dot{I} = aE - I \tag{2}$$

where $f(E) = aE - \beta E^3 + \cdots$, the lowest order of which is van der Pol equation[4], whereas in a different order estimation of E and I, Duffing type of equations will be obtained.

For a high level of activities, we get Volterra-Lotka type equations:

$$\tau_1 \dot{E} = g(E) - I + b_1 EI + P$$
$$\tau_2 \dot{I} = aE - I + b_2 EI \tag{3}$$

where $g(E) = \alpha E - \beta E^2 - \gamma E^3 + \cdots$.   The equation (3) will imply that mass action in the nervous system can be interpreted from an ecological point of view when E is regarded as "predator" and I as "prey".

The solutions of these equations have been known to exhibit limit cycle oscillations which may be deemed to represent a simplified model for the pace-maker of alpha-rhythm in EEG[4]. Analyzing the model equations in the phase plane, it is shown that an external afferent input, P, to stable qeuilibria and limit cycle oscillations of the eq. (2) and (3) gives rise to evoked responses and blockings.   Application of sinusoidally changing external input with fixed or linearly changing frequency to a generalized Duffing or van der Pol equation:

$$\ddot{E} + f(E)\dot{E} + g(E) = a \sin wt \tag{4}$$

is known to exhibit an entrainment of frequency, a hysteresis with jump in amplitude, and subharmonic oscillations[6].   Thus, the hypothesis that limit cycle oscillations of eq. (2) or (3) are the model of the pace-makers of alpha-rhythm might be verified by occurrence of these phenomena in photic evoked responses.   In terms of stochasticity of afferent input, an application of Gaussian noise $n(t)$ to the right hand side of eq. (4):

$$\ddot{E} + f(E)\dot{E} + g(E) = a \sin wt + Kn(t) \tag{5}$$

has been known to exhibit a transition between several modes in the hysteresis region and macroscopic fluctuation of amplitude and phase[6].

A more interesting case in relation to thalamo-cortical interaction is the nonlinear system with two degrees of freedom, which is perturbed by Gaussian noise:

$$\ddot{X} + a\dot{X} + w_0^2 X = kn(t)$$
$$\ddot{Y} + b(1 - Y^2)\dot{Y} + w_1^2 Y + cY^3 = X \tag{6}$$

This system is, then, known to exhibit a spontaneous mode switching and hysteresis according to the magnitude of K, and chaotic behaviors which are ascribed to the strange attractor of eq. (6)[7].   Since the input to any neural mass X always changes its magnitude K, any other neural mass Y with nonlinearity and inputs from X exhibits mode switching and chaotic behaviors which account well for a great variability of amplitude and phase of EEG.

In case of spatially interacting neural mass in homogeneous sheet, Wilson and Cowan proposed the nonlinear integro-differential equations[8]:

$$\tau_e E_t + E = (1 - r_e E) S_e [c_{ee} E * \beta_{ee} - c_{ei} I * \beta_{ei} + P_e]$$
$$\tau_i I_t + I = (1 - r_i I) S_i [c_{ie} E * \beta_{ie} - c_{ii} I * \beta_{ii} + P_i], \tag{7}$$

where "*" indicates a spatial convolution operation of delayed activities, and $\beta=b$ $\exp(-|x|/\sigma)$ indicates the connection density with other neurons:

$$E*\beta\,(x,\,t)=\int_{-\infty}^{\infty}E(y,\,t)*\beta\,(x-y)\,dy.$$

For low level of activities, Nagumo type equations can be obtained after Taylor expanding the convolution[9]:

$$\tau_1 E_t = f(E)-I+DE_{xx}$$
$$\tau_2 I_t = aE-I \tag{8}$$

where $f(E)=aE-\beta E^3+\cdots$, the spatially localized version $(D=0)$ of which is equivalent to FitzHugh type equation (2). It should be noted that the eq. (8) are model equations derived originally for a pulse transmission on the axon. By means of derivative expansion, we get a nonlinear partial differential equation for complex amplitude W of wave trains around a neutrally unstable singular point of the eq. (8)[10]:

$$W_t=(1-ia_0)W-(1+ia_1)|W|^2W+(1+ia_2)W_{xx} \tag{9}$$

This nonlinear equation is called an envelope equation for nonlinear modulation which provides an another possibility to account for a variability of amplitude and phase of EEG.

Entrainment and Hysteresis

EEG sometimes responds synchronously to the frequency of photic stimulations, and exhibits a hysteresis for a train of photic stimulations with changing frequency[11]. Since an entrainment and a hysteresis are characteristic of nonlinear systems, experimental tests for them might be used as a confirmation of the hypothesis that the pace-makers of alpha-rhythm are represented by limit cycle oscillations of the eq. (2) and (3).

As a control, a background EEG (35 sec) of one subject (normal male, 34, monopolar recording at 0_1, sampling frequency 100 Hz) is analyzed. Fig. 1 shows band pass wave forms and their envelopes of background EEG by complex demodulation[12]. Fig. 2 shows contour map of power spectrum of background EEG. Fig. 3 shows phase changes[12] of band pass wave forms of Fig. 1. (Throughout this paper, Fourier spectrum is calculated by FFT algorism. The flow chart is shown to the right of this page. In TAPER, a single 1 sec time base of 102 points is extended to 124 points by packing of 22 zeros.)
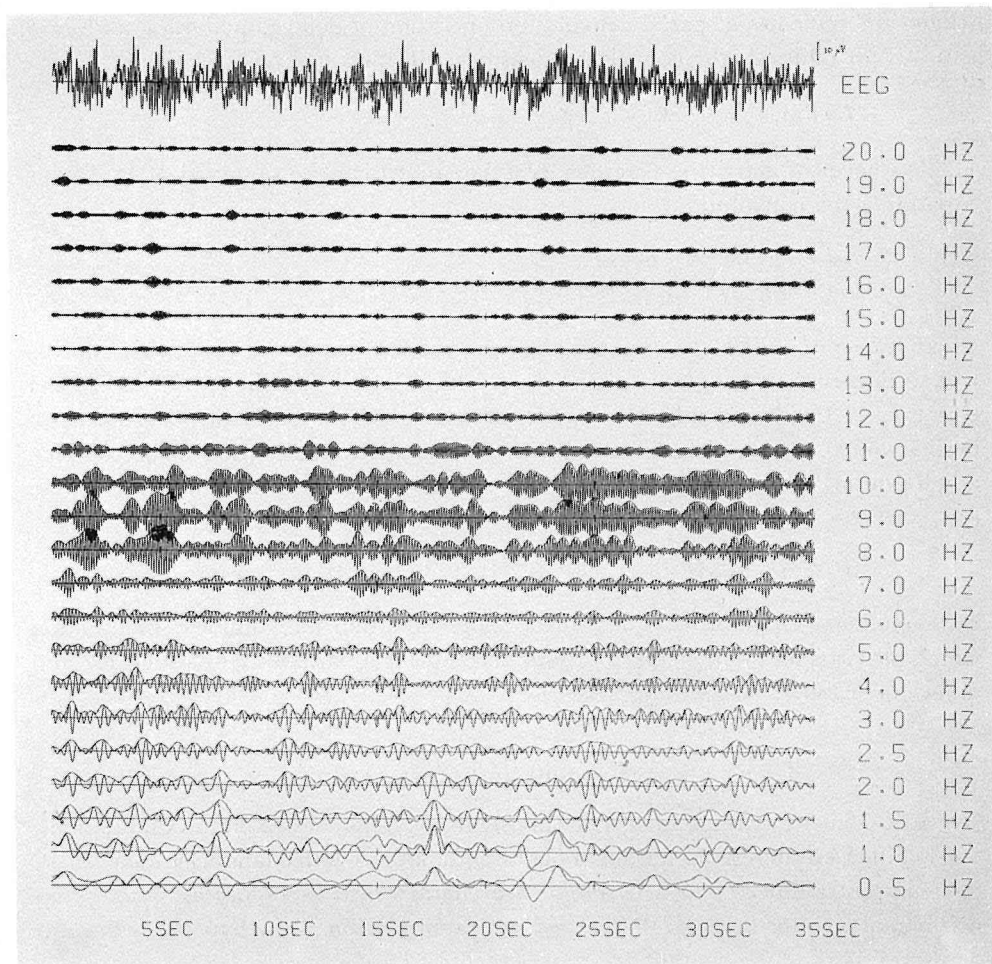
DATA
↓
TAPER
↓
FFT
↓
SPECTRUM
↓
HANNING
↓
GRAPH
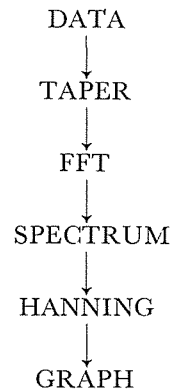
Figure 1.   Band pass wave forms and their envelopes of the background EEG
            by complex demodulation.   10 μV calibration is applicable for all
            the channels.

In this EEG record, the alpha-rhythm is dominant, and it exhibits periods o
a great variability as well as a marked stability of the oscillation.   Compared with
the other bands, its phase hardly changes.   Thus, the alpha-rhythm appears to
behave as an independent limit cycle oscillation and twist the other bands.   These
observations seem to confirm its subcortical origin.   The cortical tissue might be a
passive network driven by exogeneous alpha-rhythms.   The lower deltaband activity
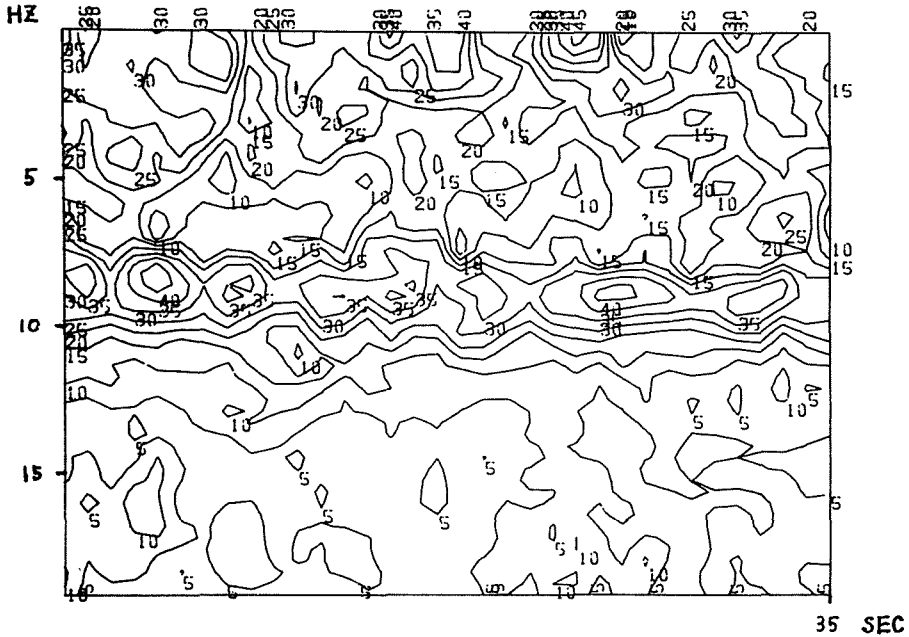(lower than 3 Hz) seems also to have subcortical origins because of its large amplitude

Figure 2. Contour map of power spectrum (in DB) of the background EEG.

and small phase change.   Several explanations could be found for the great vari-
ability of these bands such as intermittent synchronizations, mutual entrainments,
mode switching, chaotic behaviors due to strange attractor, and nonlinear modula-
tions.   The origin and function of the great variability remain, however, unsolved
so far.

Fig. 4 shows a typical EEG record and band pass wave forms of the same subject
for a train of photic stimulations with linearly changing frequency started from 1 Hz
to 20 Hz.   Fig. 5 shows a record of the photic stimulation, starting from 20 Hz
and down to 1 Hz.   Fig. 6 and 7 show the contour maps of power spectra of Fig. 4
and 5, respectively.

From these figures, several conclusions can be drawn:

(1)   No hysteresis can be distinguished in the external frequency range of 8–13 Hz,
whereas marked differences in power are noticeable in the external frequency
range of 1–5 Hz (high in going, low in coming) and 15–20 Hz (low in going,
high in coming).   The former can be ascribed to onset VER in going and attenua-
tion by habituation in coming.   The latter can be ascribed to the subject's aware-
ness of frequency pattern change in coming, for the photic stimulations in Fig. 5
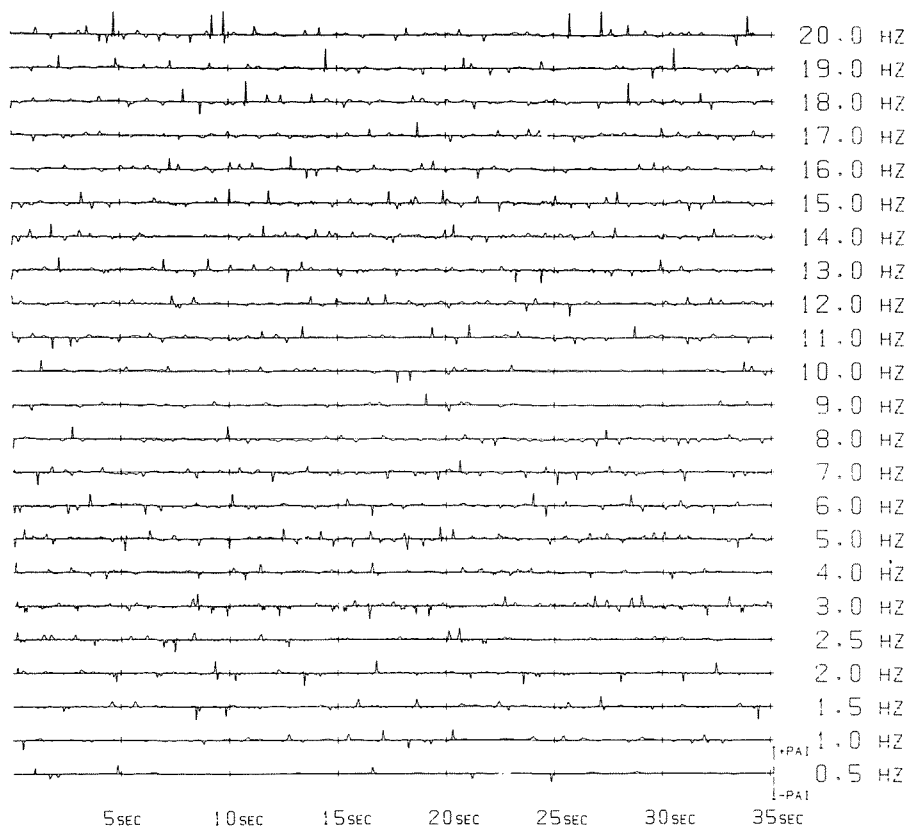start just after the last flash in Fig. 4 without any pause.

Figure 3. Phase changes of band pass wave forms of Figure 1. The calibration
is shown in radian at the bottom to the right of this figure.

(2)   In comparison with the control EEG, the amplitudes in Fig. 4 and 5 are sup-
pressed, but the stochastic variability has remained intact.

(3)   The differences in the experimental conditions between the author's and Dr.
Kawabata's[11] who showed clearly the existence of hysteresis in the range of alpha-
band, are (i) a single raw record vs. an average of 32 trials, (ii) speed of
linearly changing frequency of photic stimulation: 0.3 Hz/sec vs. 0.5 Hz/sec,
(iii) going-coming paradigm vs. going and coming, separately, (iv) masking
effects of some uncontrollable mental processes, and (v) subject. Among these,
(i) and (v) appear to be vital.

(4)   The hypothesis in the preceding section requires further detailed experiments
for confirmation. For the model to be "universal", the model for alpha-rhythm
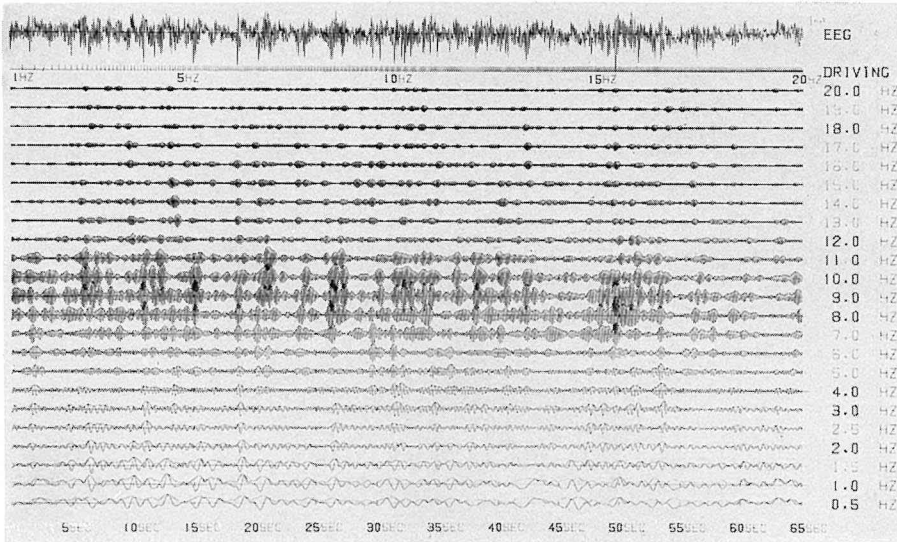must install in itself the stochastic variability and the subject dependence.

Figure 4. Band pass wave forms and their envelopes of the EEG record for a train of photic stimulations with linearly changing frequency from 1 Hz to 20 Hz.
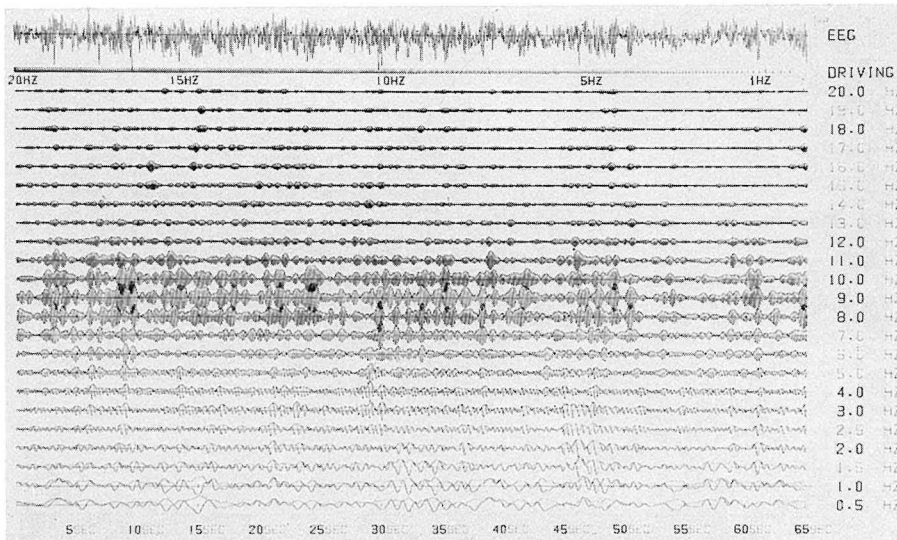

Figure 5. The same tracing as Figure 4 of the reverse process from 20 Hz to 1 Hz. The photic stimulation starts without pause just after the last flash in Figure 4.
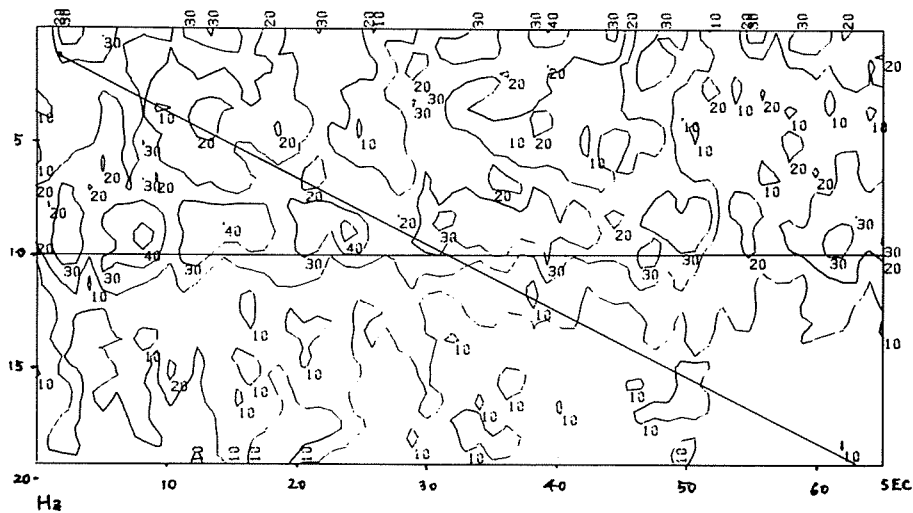
Figure 6. Contour map of power spectra of Figure 4. The diagonal line shows
the frequency of photic stimulations. The number shows the spectral
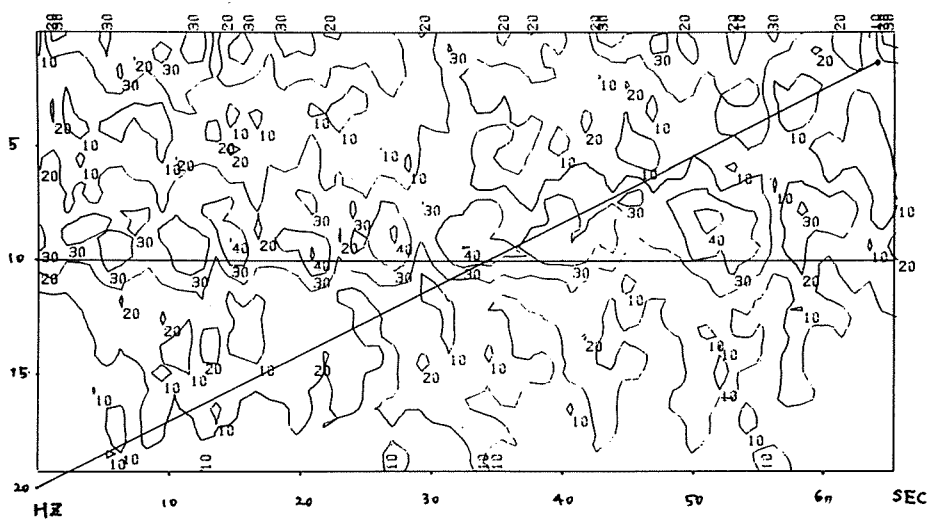intensity at $\mu V^2/sec/Hz$.

Figure 7. Contour map of power spectra of Figure 5. The diagonal line shows
the frequency of photic stimulations.

Spectra of VER

As a preliminary step for a study of event-related changes in the cortical rhythmic activities, we have analyzed visual evoked responses (VERs) produced by a random flashing by means of Fourier spectra (power and phase spectrum, bispectrum, bicoherence and biphase). EEG records of 2.5 sec are divided into 5 intervals of 500 msec: [1]–[5]. A flash is given to the subject at the beginning of the second interval. The subject is a normal male 34 years old, whose EEG is recorded from O_1 monopolally at 200 Hz. The frequency resolution is about 1.6 Hz because there is one axis of symmetry in the figures of bispectrum, bicoherence and biphase.

Fig. 8 shows 50 VERs (#1–#50), the ensemble averaged VER (#51) of 50 VERs, and their power spectra. Fig. 9 shows the phase histograms of 50 VERs. Fig. 10, 11 and 12 show the enzemble averaged mean, standard deviation (S.D.) and the coefficient of variation (C.V.=S.D./mean, where mean is replaced by (mean+180°) in cases of phase and biphase because these are defined in [−180°, +180°]) of 50 spectra, respectively. Fig. 13 shows the spectra of the ensemble averaged VER (#51).

From examination of these figures, several conclusions can be drawn:

(1) Ensemble averaged VER (#51)

The ensemble averaged VER is shown at the bottom of Fig. 8, and its enlargement is given below:
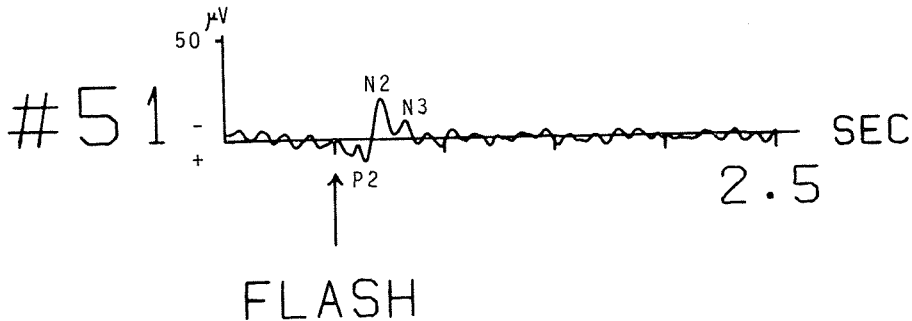
The latencies (in msec) of the positive and negative peaks in [2] of #51 zre listed below:

PEAK	P1	N1	P2	N2	P3	N3	P4	N4
LATENCY	80	110	150	230	275	340	385	420

(2) Power spectrum

The mean and S.D. of power spectra suggest that in general the alpha-band
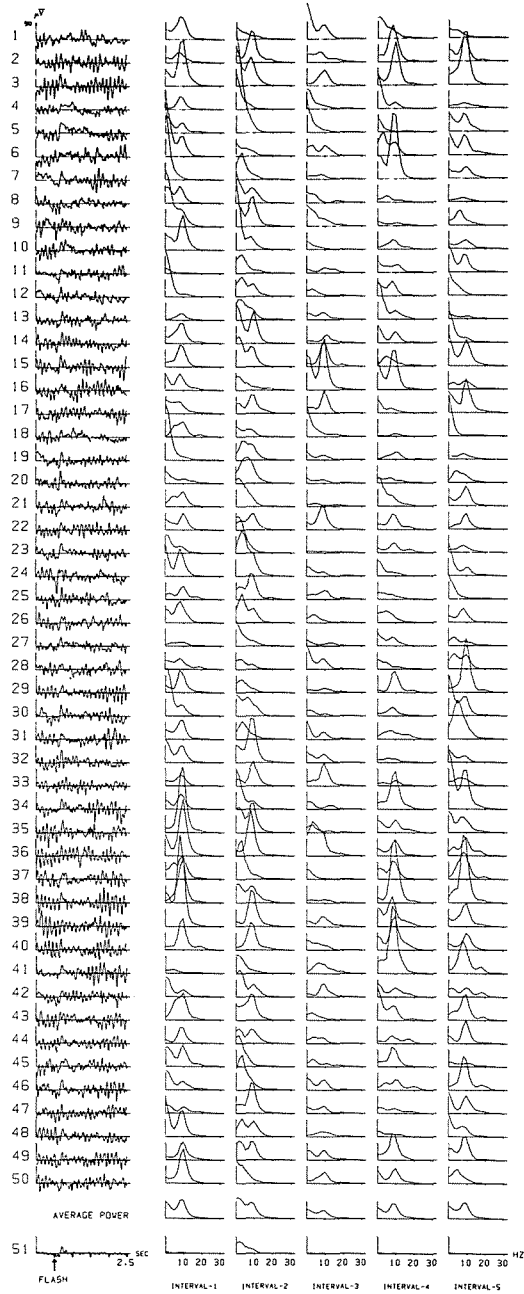
Figure 8.   50 VERs for a random flashing, their power spectra and the ensemble averaged
           power spectrum (not in DB) in the 5 intervals (500 msec). The 51st is the
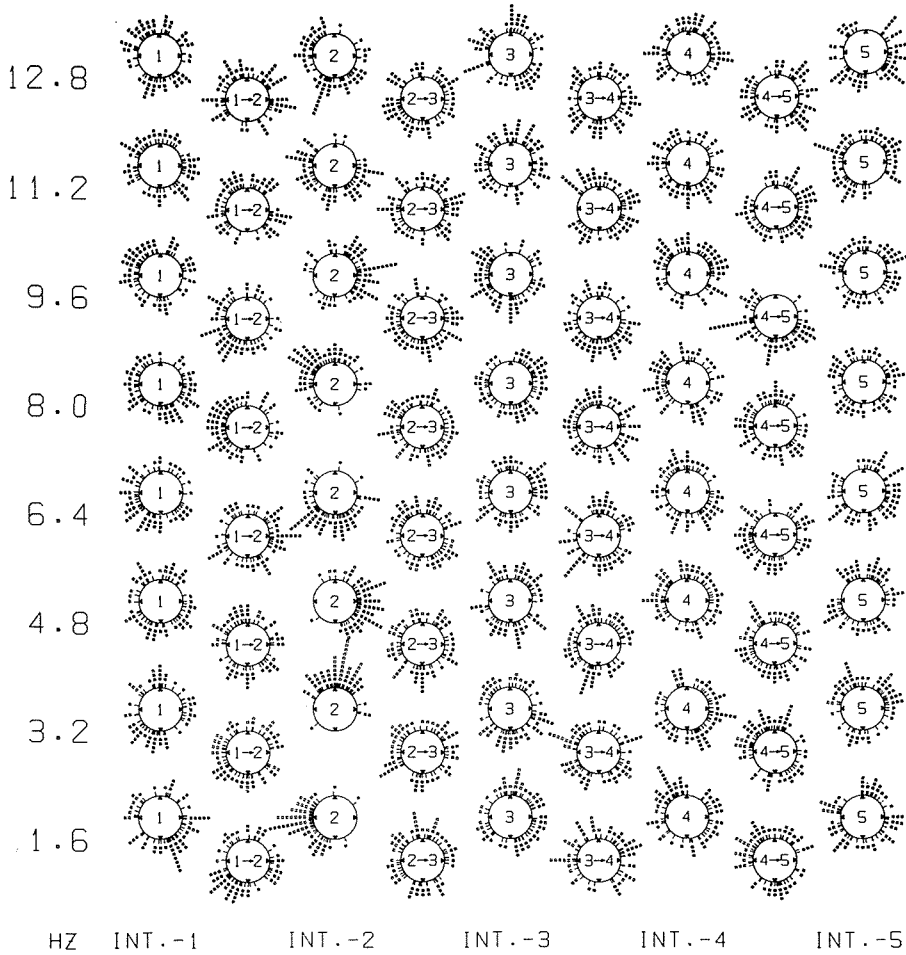   ensemble averaged VER and its power spectrum.

Figure 9.   Phase histogram of 50 VERs

A phase angle θ (f, N, I) of the Fourier component with frequency f of Nth data in the interval [I] is sorted into 36 classes with 10 Deg. width:

[10 $k-15$, 10 $k-5$) $k=1$, 2, 3, .. , 36.

and their histograms are plotted around a circle with the symbol I.

The symbol $I \rightarrow I'$ in a circle indicates the scattering phase histogram from [I] to [I']: θ (f, N, I)$-\theta$ (f, N, I).

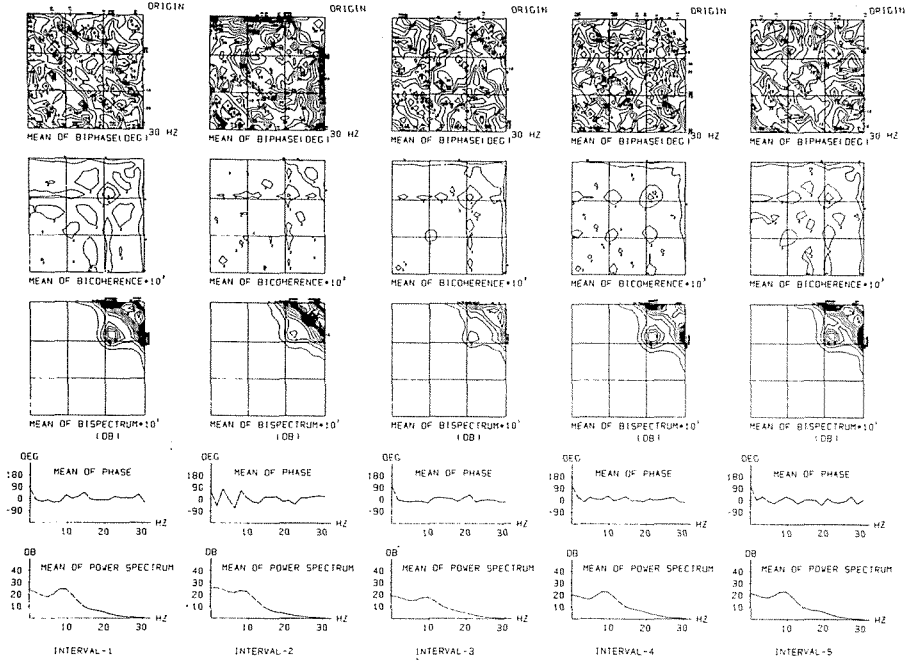The angle is defined as east$=0°$, north$=90°$, west$=\pm 180°$ and south$=-90°$.

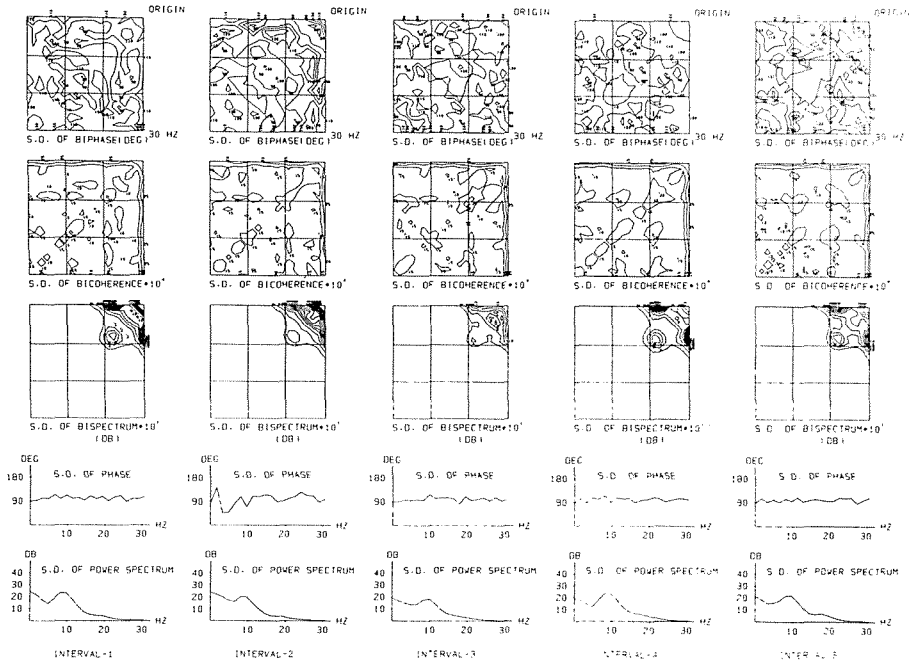Figure 10.   Mean of 50 spectra in 5 intervals.

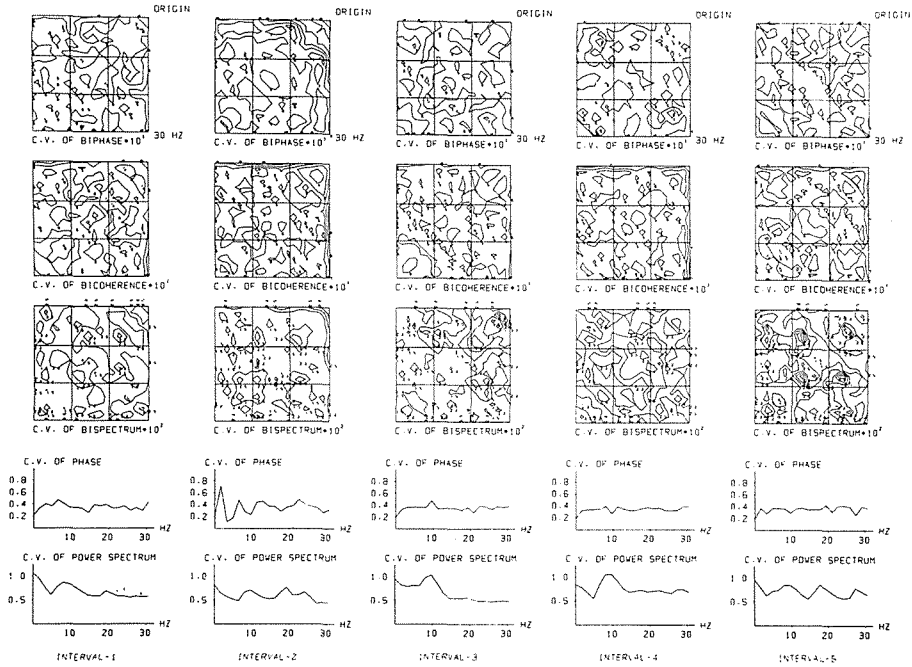Figure 11.   Standard deviation (S.D.) of 50 spectra in 5 intervals.

Figure 12. Coefficient of variation (C.V.) of 50 spectra in 5 intervals.
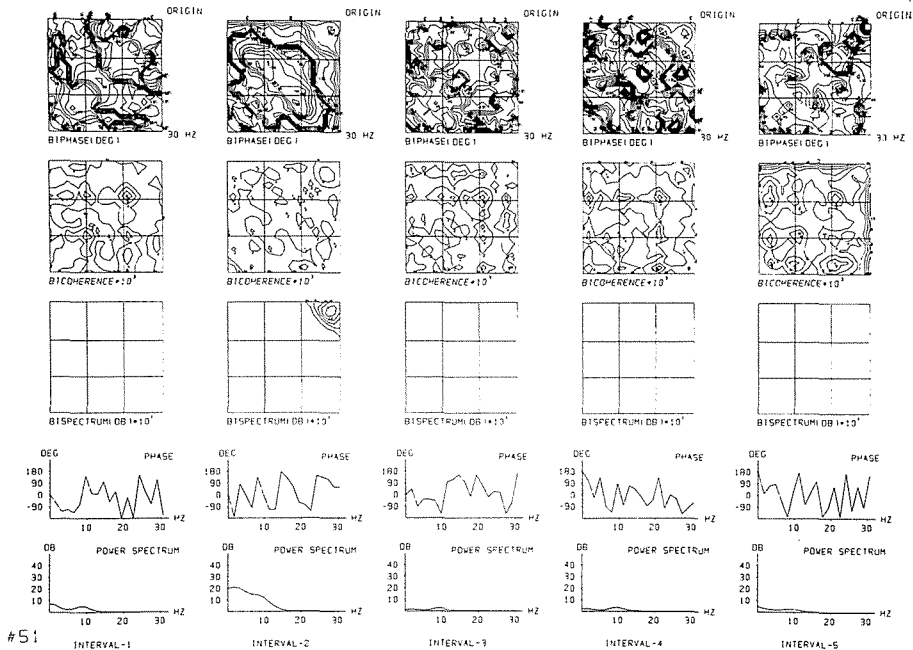
Figure 13. Spectra of the ensemble averaged VER in 5 intervals.

activities begin to attenuate in [2], and come to a state of blocking in [3], then go into recovery processes in [4]. The contrast between a small C.V. in [2] and a large C.V. in [3] suggests the existence of deterministic components time-locked to the stimulus in [2], which is also confirmed in phase spectrum. Because of the great variabilities in amplitude and phase, there are great discrepancies between the spectrum of ensemble averaged VER (♯51) and the ensemble mean of 50 spectra (Fig. 8). The common spectral features are found only in the frequency range lower than 12.8 Hz in [2], during which interval we have a VER mainly composed of deterministic components locked to the stimulus.

(3)　Phase spectrum

Because of the periodicity of phase angle in the domain of [180, +180], the real statistical features of phase distribution cannot be understood by the ordinary statistics, such as mean, S.D. and C.V.. Inspecting the phase histograms in Fig. 9, the phases in [2] of the frequency range lower than 12.8 Hz are seen to be locked in the intrinsic phases which coincide with the phases in [2] of the ensemble averaged VER (♯51) in Fig. 13 as tabulated below (degree):

Frequency	1.6	3.2	4.8	6.4	8.0	9.6	11.2	12.8	Hz
Phase in Fig. 8	−170	80	−10	−90	140	10	−100	−120	Deg.
Phase in Fig. 13	−170	90	−5	−95	140	0	−110	−110	Deg.

(Phases in Fig. 13 are median values rounded to a multiple number of 10 Deg.)

The phases in the other intervals, however, are scattered and show a random distribution, except for 9.6 Hz whose phase holds its angle around a specified value until the end of the interval [4]. The outstanding feature of the table is the clockwise phase shift by −90 degrees. The phases of 4.8 and 9.6 Hz are approximately zero. It is a consequence of the rapidly increasing long slope from P2 to N2, for its zero crossing latency is approximately 208 msec (=1000/4.8). The summation of the phases of 3.2 and 6.4 Hz coincides with the phase of 4.8 Hz. This suggests that the composition of the Fourier components of 3.2 and 6.4 Hz is a modulation of the Fourier component of 4.8 Hz. This statement is, however, valid only under a condition that the two components have the same amplitude, but becomes less valid as such condition is not met exactly.

The similar situations are observed on the phases of 1.6 and 8.0 Hz in reference to 4.8 Hz, and on the phases of 8.0 and 11.2 Hz in reference to 9.6 Hz. The antisymmetry of phase about 4.8 Hz and 9.6 Hz suggests the existence of a sum rule for phases around 4.8 Hz and 9.6 Hz, which is a direct evidence of a strong correlation between the two phases. This, in turn, seems to show an existence of neuronal control mechanisms of evoked responses common to the alpha-rhythm in the neuronal arborization of the cerebral cortex and the cortical excitability. In the context of

information processing, the facts that the cortical excitability has a specific affinity to the frequency of alpha-band and its harmonics in case of VER as well as background EEG, and that the co-existence in [2] and the simultaneous attenuation in [3] of the alpha-rhythm and VER, suggest the functional significance of the alpha-rhythm in the early stage of the information processing in the thalamo-cortical system, where a hypothetical "scanner" might perform a scanning of the information flux from periferal sensory organs[13] with neuronal adaptation of the central nervous systems.

(4) Bispectrum and bicoherence

As is well known[14], a Gaussian process $X(t)$ is expressed as a linear combination of infinitely many independent components, and its bispectrum $B(f_1, f_2)$ is always zero, whereas $B(f_1, f_2)$ of a weakly non-Gaussian process $X(t)$ is not necessarily zero. The non-zero $B(f_1, f_2)$ is a direct measure of the second order nonlinear interaction between three modes of Fourier components whose frequencies are f_1, f_2 and $(f_1 + f_2)$, and its statistical significance must be confirmed by the estimated bicoherence.

For brevity, we make use of abbreviations hereafter for frequency bands as schematized in the below:

$$\overset{\leftarrow \delta_1 \rightarrow}{\underset{0}{\vdash}} \overset{\delta_2}{\underset{3\ 4}{\dashv}} \leftarrow \theta \longrightarrow \overset{\leftarrow \alpha_0 \rightarrow}{\overset{}{\times \alpha_1 \times}} \overset{}{\underset{8\ 9\ 10\ 11}{-\alpha_2-}} \overset{}{\underset{13}{\times}} \cdots \beta_1 \overset{\leftarrow \beta_0 \rightarrow}{\underset{19\ 20\ 21}{\times}} \beta_2 \overset{\leftarrow \gamma_0 \rightarrow}{\underset{24\ 25\ 26}{\times}} \overset{}{\underset{30}{\gamma_1}} \overset{}{\longrightarrow} Hz$$
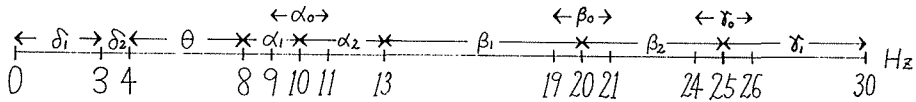
Several peaks in the contour maps of mean, S.D. and C.V. of bispectra are listed below:

	INTERVAL				
	[1]	[2]	[3]	[4]	[5]
MEAN	$\delta_1-\theta-\alpha_1$	$\delta_1-\delta_1-\delta_2$		$\delta_1-\theta-\alpha_1$	$\delta_1-\theta-\alpha_1$
and	$\delta_1-\delta_1-\delta_2$	$\delta_2-\delta_2-\theta$			$\delta_1-\delta_1-\delta_2$
S.D.	$\delta_2-\delta_2-\theta$				
C.V.			$\delta_2-\theta-\theta$		$\theta-\beta_1-\gamma_0$
$\geqq$					$\beta_1-\beta_1-\gamma_2$
0.035					$\theta-\theta-\alpha_0$

(The peaks in MEAN and S.D. are greater than 1 DB. The peaks in the table are listed in the order of magnitude. γ_2 is the frequency range of [30, 35].)

Marked differences between mean, S.D. and C.V. can be seen in the table.

Mean and S.D. are quite dependent on the exogenous components and their variabilities. C.V. is not dependent on the exogenous variabilities, but it depends on the endogenous reaction in the neuronal networks caused by the exogenous.

Thus, the several peaks of C.V. in [3] and [5] might be considered to reflect a neuronal mechanism of information processing, such as discrimination or comparison, registration or retrieval, analysis or synthesis, and set or reset of the neuronal machine.

The peaks of mean and S.D. except for in [2] are not observed in the bispectrum of the ensemble averaged VER ♯ 51, for these are cancelled out by the variabilities of amplitude and phase.

As for the bicoherence, it reveals quite different features from bispectrum, that is, the predominance of alpha-band and its higher harmonics, the typical pattern of which can be seen in the contour map of mean of bicoherence (Fig. 10) and similar pattern in the ensemble averaged VER ♯51, whereas no peak in the mean of bicoherence is higher than the 95% significance level: 0.09748. Since the statistical evaluation for significance level requires the stationarity of the time series, it is applicable to the interval [1], but not to the other intervals, because VER assumes an event of the nonstationarity in principle. Therefore, any significance test of VER analysis may not be reliable from a theoretical point of view, but will be useful as an auxiliary.

(5) **Biphase**

A biphase (f_1, f_2) is defined as follows:

$$\text{biphase } (f_1, f_2) = \text{phase}(f_1) + \text{phase } (f_2) - \text{phase } (f_1 + f_2).$$

Since the real features of biphase distribution cannot be grasped by mean, S.D. and C.V. as mentioned previously in the section "(3) Phase spectrum", and the 3-dimensional diphase histogram of 50 VERs cannot be easily drawn, we must be contented with a visual inspection of the ensemble average ♯51 for the present stage of analysis.

Because the contour line is drawn at every 45 degrees, a jump through 4 contour lines signifies out of phase, and a jump through 8 contour lines signifies in phase. When we pass through a narrow boundary region densely packed with severa parallel contour lines, we are to meet a drastic biphase change. In order to show specific compact boundary regions, and to make their interpretation easy, we have prepared a new terminology:

(i)   SPEC (f_0) in $[f_1, f_2]$: a strip region parallel to the horizontal or the vertical axis, defined by $f = $ constant f_0 in the interval $[f_1, f_2]$,

(ii)   SUMS (f_0) in $[f_1 \times f_2]$: a strip region perpendicular to the symmetry axis, defined by $f_1 + f_2 = $ constant f_0 in the rectangular region $[f_1 \times f_2]$,

(iii) DIFF(f_0) in $[f_1 \times f_2]$: a strip region parallel to the symmetry axis, defined by $f_1 - f_2 = $ constant f_0 in the rectangular region $[f_1 \times f_2]$,

and, for an extensive region with constant value and a narrowly limited region like a spot:

(iv)   AREA (phase) in $[f_1 \times f_2]$,

(v)   SPOT (phase) in (f_1, f_2),

where f denotes either frequency or frequency band.

In the biphase spectrum of ♯51 in the interval [2], there are AREA(0°) in the two right isosceles rectangles $[0 \leq f_1 + f_2 \leq a_0]$ and $[f_1 + f_2 \geq \gamma_0, f_1 \text{ and } f_2 \geq 17.2$, and a great "volcano with a crater" surrounded by a "somma" which is a linkage of several specific regions: SUMS (8.0) in $[a_1 \times a_1]$, SPEC (8.0) in [11.2, 17.6], SPEC (6.0) in β_0, SUMS (γ_0) in $[\theta, \beta_1]$, SPEC (θ) in γ_2, SPEC (28.8) in $[\theta, a_0]$, SUMS (40.0) in $[a_2 \times \gamma_1]$, SPEC (γ_0) in β_1, SPEC (16.0) in γ_1, SPEC (28.8) in β_1. These biphase structure is considered to be characteristic of a VER time-locked to a photic stimulus.

So far, the alternative efforts to discriminate a biphase process in VER by the multivariate statistical analysis of 50 biphase patterns (♯1–♯50) have not succeeded due to its great variabilities.

Triplet Versus Singlet Paradigm

Several authors have reported that there are (1) emitted potentials, similar to evoked responses, time-locked to the stimulus which is expected but absent, and (2) negative deflections, similar to the CNVs. These authors have discussed their possible functional significance in relation to the cortical excitability and information processing in the central nervous system[15–19].

In order to analyze the emitted potentials and the negative deflection in the frequency domain, we have employed a triplet versus singlet stimulation paradigm (Fig. 14). In this paradigm, triplet mode A (triplet flashes with the same interval $\tau = 500$ msec) and singlet mode B (a single flash) are generated randomly (the ratio A/B=5/1) with random inter "mode" intervals $\{t_n : n = 1, 2, 3, \cdots\}$. The photic stimulations were presented to the subjects (normal and unconscious) without any discrimination task. Averages of 20 VERs for A and B are obtained, and then they are compared with a control wave form (an average of 20 VERs for a random flashing). An example is given in Fig. 15 (normal male, 34, O_1–A_1).

Compared with the control, the emitted potentials can be seen as the 4th and 5th responses in the triplet, and the 2nd response in the singlet, and a slow negative shift in the singlet. 12 VERs for the triplet versus singlet paradigm, and their power and phase spectra in each interval are shown in Fig. 16 and Fig. 17.

Subjects ♯5,6 was unconscious, but they understood some directions by a doctor, such as "lift your hands", because of their efforts to lift their hands a bit. Subjects
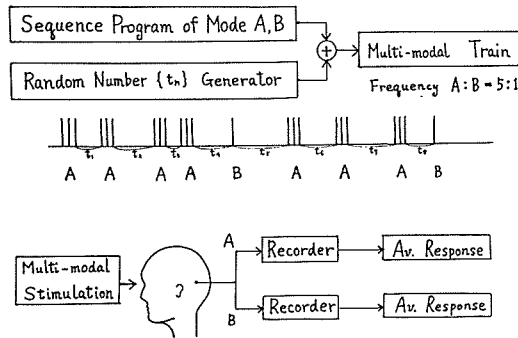
Figure 14. Triplet versus singlet paradigm.

♯ 7,8 were comatose due to injuries after a traffic accident.   This study was done a
month after the operation.   They had recovered two months after the experiment.
Subjects ♯ 9,10 have been reduced to a vegetable state.   Among these, spectra of
♯ 1 and ♯ 2 are shown in Fig. 18 and Fig. 19.

From analyses of these figures, we get several results:

(1)   Time   domain   analysis

The emitted potentials for this paradigm are observed both in the normal and
unconscious, whereas the negative deflection has appeared often in the normal and
only rarely in the unconscious.   These two potentials are predominant in the
anterior than the posterior region on the scalp.   The emitted potential is a retarded
evoked response, whose components are loosely time-locked to the expected stimulus,
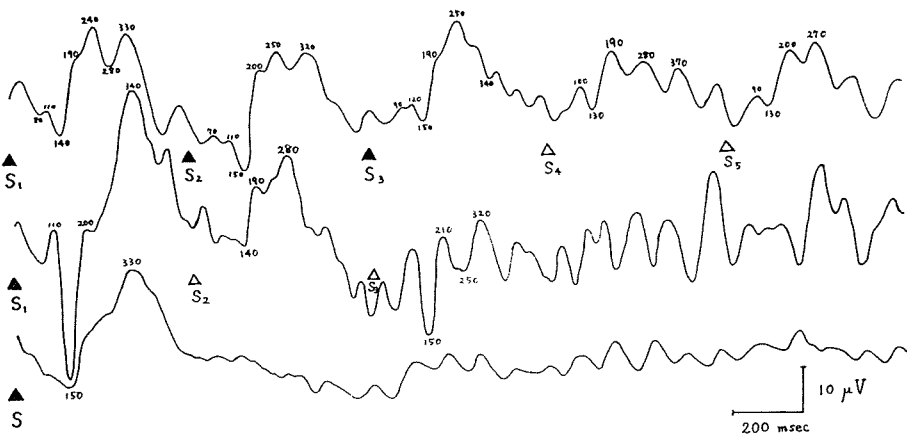

Figure 15. A typical VER for the triplet (upper), the singlet (middle) and the
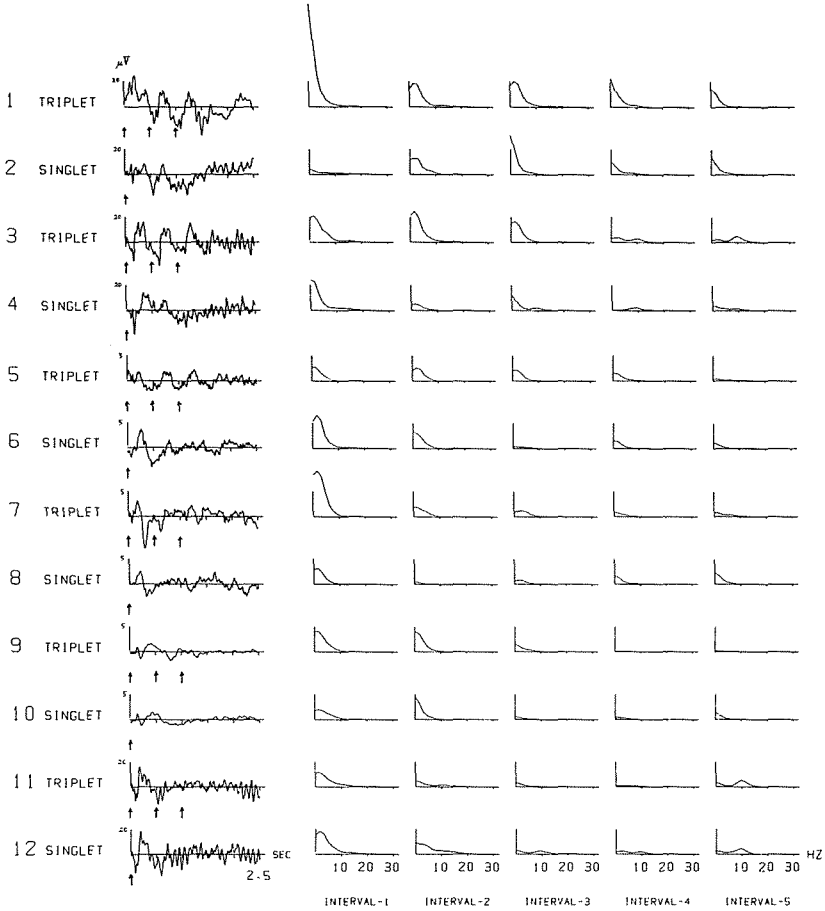   control (bottom).

Figure 16. 12 VERs for the triplet versus singlet paradigm and their power
spectra (not in DB) in 5 intervals.

Subject	1, 2	:	normal male 34	F_{p1}–A_1
Subject	3, 4	:	normal male 34	P_3–A_1
Subject	3, 6	:	unconscious male 19	O_1–A_1
Subject	7, 8	:	unconscious male 21	O_1–A_1
Subject	9,10	:	unconscious male 67	O_2–A_2
Subject	11,12	:	normal male 19	O_1–A_1

The VERs of ♯3 and ♯4 are the same VERs in Figure 15.

and hardly occurs when the negative deflection is dominant, and when we set the
interval τ of the triplet flashes shorter than 333 msec (3 Hz). Therefore, they are
considered to be an evoked response in the cerebral cortex elicited by a temporal
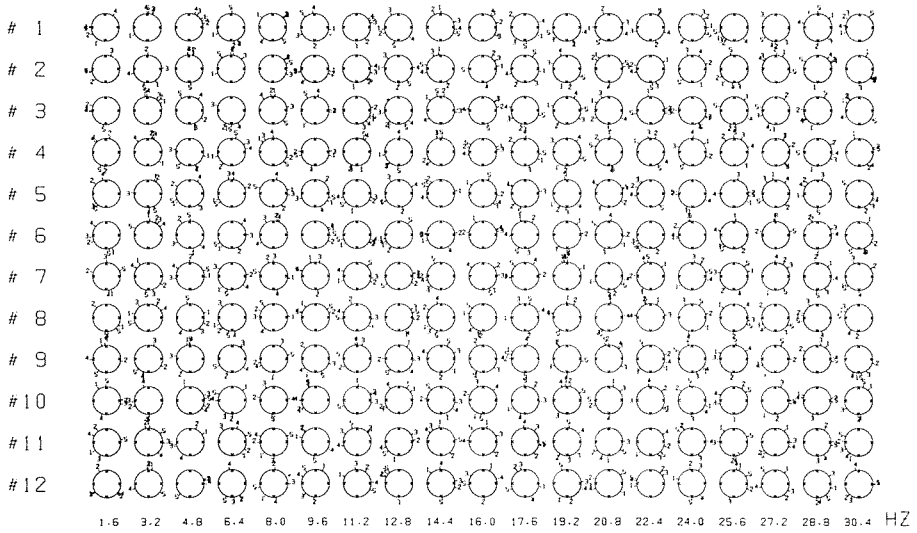conditioning of the triplet timing in the thalamus. A timing mechanism built in the

Figure 17.   Phase spectra of 12 VERs in five intervals.   The number I around
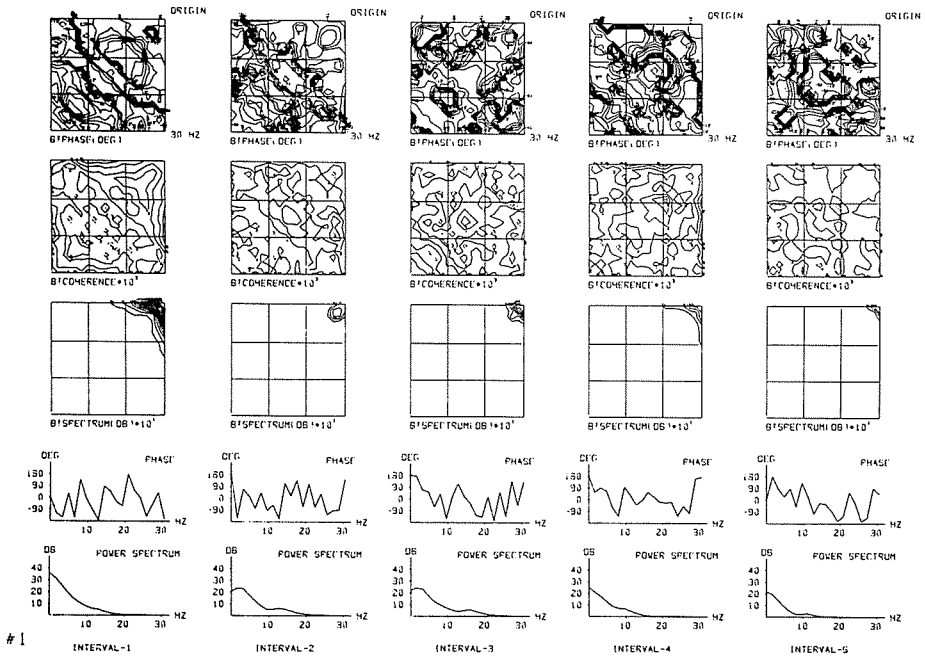a circle indicates the phase angle of the Fourier component in the
interval [I].

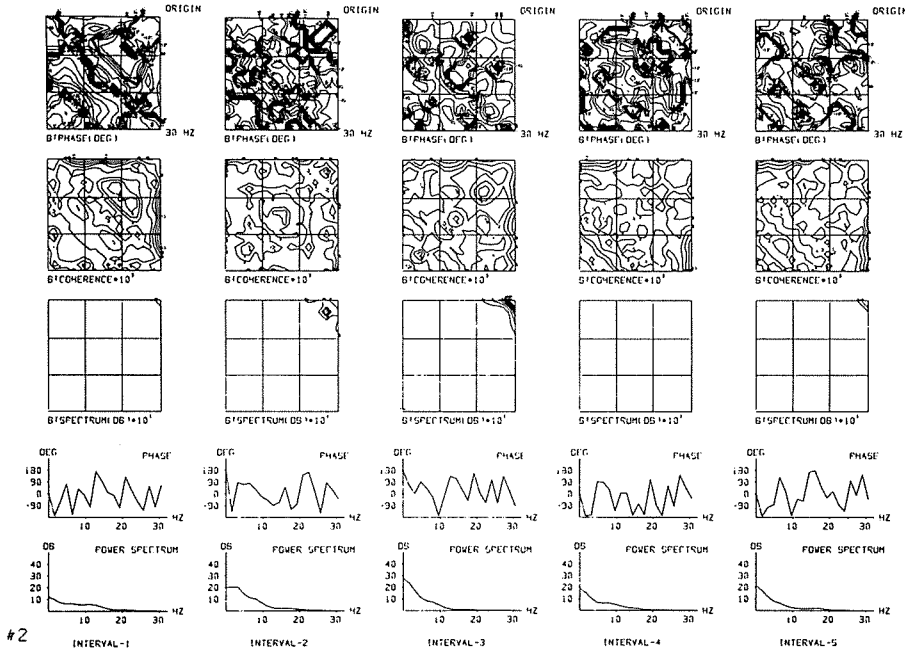Figure 18.   Spectra of ♯1 (triplet) in 5 intervals.

Figure 19. Spectra of ♯2 (singlet) in 5 intervals.

thalamic neural mass works in cooperation with the frontal cortex through the thalamo-cortical circuit when an attention makes the cerebral cortex ready to distinguish what the paradigm is.

Since the negative shift is related to the arousal level as well as attention, and antagonistic to the occurrence of the emitted potentials. It has a positive correlation with the habituation of VERs for triplet.   Its roots are considered to be found in the midbrain reticular system and its function is to make the cerebral cortex sensitive to any change in the paradigm.   VERs for a train of periodically repetitive stimulations are suppressed because the stimulations have little information[15,16).   The relation between the CNV and the negative shift is left unsolved in this paper. (Is CNV the enhanced version of the negative shift by the motivation to make a motor action in response to the imperative stimulus or not?   Does CNV consist of multi-components?)   The extension from triplet to quartet, quintet, ..., ten flashes and so on has been observed to bring about much more complex responses with less reproducibility.   We don't know whether a stimulation with fewer than quintet produces a highly reproducible responses because of the timing mechanism built in the central nervous system, or because of a sense of rhythm learned later in our lives through music.

(2)   Frequency domain analysis

The phase histogram (Fig. 17) shows the remarkable fact that not only the triplet (♯odd) but also the singlet (♯even) give rise to a biased phase distribution, that is, several Fourier components keep their phases constant during some intervals.   We would like to call it an "event related phase preservation (ERPP)".

(i)   In the frequency range lower than the alpha-band ($\leqq 12.8$ Hz):

As analyzed in the preceding section, a flash causes a phase-locking of the Fourier components lower than the alpha-band in the first interval of 500 msec length after the flash, whereas in the next interval phases are scattered randomly.   Though we have not analyzed their intrinsic phases of frontal pole VER (♯1, 2) and parietal VER (♯3, 4) [occipital VER in the preceding section], it is certain that ERPP serves for a formation of the emitted potential.

(ii)   In the frequency range higher than the alpha-band (>12.8 Hz):

Since we have not observed ERPP in the occipital VER with a random flashing paradigm and the Fourier components in this frequency range do not serve effectively for a formation of VER, the ERPP in this range is considered to be related to the cognitive mechanism.   Thus, the coherent phases in β and γ bands might play a role of a detector which detects perturbation and analyses the information in it.   The specific structures found in biphase (Fig. 18 and 19) are the direct consequences of the ERPP.   Among those, outstanding features characteristic of this paradigm are the progressive evolutions of the specific boundary regions: DIFF (1.6), DIFF (3.2), DIFF (4.8), DIFF (9.6), DIFF (20.8) from the low frequency range to the higher, which are the alternative expressions of the scanning.   Finally, it is worth mentioning that SUMS (greater than 30) in bicoherence develops during the negative deflection as we see in the interval [4], [5] of ♯2 (Fig. 19).

Summary and Discussion

A frequency domain analysis (FDA) of the event related responses in EEG has been presented in which its effectiveness has been demonstrated as complementary to a time domain analysis (TDA).

Several problems are, however, left unsolved:

(1)   FDA is much more sensitive to the variability of time series than TDA,

(2)   the validity of FDA of the essentially nonlinear wave,

(3)   the statistics of phase and biphase, and

(4)   the physical relationships between a phase change in FDA of EEG and a phase change recorded by a physiological laminar analysis[20].

Acknowledgements

References

1) Freeman, W. J. (1975)   Mass Action in the Nervous System, Academic Press, New York.
2) Wilson, H. R. and Cowan, J. D. (1972)   Biophys. J., 12, 1.
3) FitzHugh, R. (1961)   Biophys. J., 1, 445.
4) Nogawa, T. et al. (1976)   Digest of 11th Int. Conf. on Med. & Biol. Eng., Ottawa, 546; (1977) Electroenceph. clin. Neurophysiol., 43. 543.
5) Dewan, E. M. (1964)   J. Theor. Biol., 7, 141.
6) Hayashi, C. (1964)   Nonlinear Oscillations in Physical Systems, McGraw-Hill.
7) Ueda, Y. (1978)   Trans. I.E.E. Japan, 98-A, 167.
8) Wilson, H. R. and Cowan, J. D. (1973)   Kybernetik, 13, 55.
9) Nagumo, J. et al. (1962)   Proc. IRE, 50, 2061.
10) Nogawa, T. et al. (1977)   Proc. 30th Ann. Conf. Eng. Med. Biol., 80.
11) Kawabata, N. (1968)   Electroenceph. clin. Neurophysiol., 25, 449.
12) Nogawa, T. et al. (1976)   Electroenceph. clin. Neurophysiol., 40, 78.
13) Elul, R. (1972)   Int. Rev. Neurobiology, 15, 227.
14) Huber, P. J. et al. (1971)   IEEE Trans. Audio Electroacoust., AU-19, 78.
15) Sutton, S. et al. (1967)   Science, q155, 1436.
16) Klinke, R. et al. (1968)   Electroenceph. clin. Neurophysiol., 25, 119.
17) Barlow, J. S. (1969)   Electroenceph. clin. Neurophysiol., 27, 544.
18) Weinberg, H. et al. (1974)   Electroenceph. clin. Neurophysiol., 36, 449.
19) Simson, R. et al. (1976)   Electroenceph. clin. Neurophysiol. 40, 33.
20) Lopes da Silva, F. H. and Storm van Leeuwen, W. (1978)   Architectonics of the Cerebral Cortex, edited by Brazier, M.A.B. and Petsche, H., Raven Press, pp. 319–333.